Research & Reviews in Electrochemistry
ISSN: 0974-7540

Research and Reviews in Electrochemistry

Review | Vol 8 Iss 1

(N^{3-}, M^{5+}) Co-Doping Strategies for the Development of TiO_2-Based Visible Light Catalysts

Qingbo Sun, Bethany R McBride and Yun Liu*

Research School of Chemistry, The Australian National University, Canberra, Australian Capital Territory, 2601, Australia.

***Corresponding author:** Yun Liu, Research School of Chemistry, The Australian National University, Canberra, Australian Capital Territory, 2601, Australia, Tel: 61261251124; E-mail: yun.liu@anu.edu.au

Received: April 07, 2017; **Accepted:** June 22, 2017; **Published:** June 30, 2017

Abstract

(N^{3-}, M^{5+}) co-doping is an efficient strategy to activate the visible light catalytic behavior of TiO_2 for broad use in wastewater purification, air cleaning, hydrogen generation, and sterilization. Here, we briefly review the recent progress of (N^{3-}, M^{5+}) co-doping strategies for the development of TiO_2-based visible light catalysts. The designed synthesis methods, the characterized material properties, the measured photocatalytic activity and the introduced local defect structures are summarized. It is expected that this mini review can build up a general framework for future/current research into (N^{3-}, M^{5+}) co-doped TiO_2 materials and provide a direction for the further development of TiO_2-based visible light catalysts.

Keywords: Photocatalysis; Solar energy; Doping

Introduction

The development of TiO_2-based visible light catalysts (VLCs) is significant to enhance the utilization efficiency of clean/renewable solar energy, and to remedy the current state of environmental pollution by directly harnessing sunlight to drive a range of chemical reactions. These chemical reactions include generating hydrogen from water, removing organic/toxic compounds in wastewater or air, automatically decomposing plastic rubbish, and even sterilization. In principle, the light energy absorbed by TiO_2-based VLC materials is used to generate electrons and holes. These photo-excited carriers subsequently migrate to the surfaces of VLC materials and chemically react with various targets. This simple photocatalytic process depends on three critical steps: (1) the light absorption ability of TiO_2-based VLCs. It determines how much photo-energy can be efficiently utilized by VLCs; (2) the efficient separation of electron-hole pairs. This dictates the numbers of active reductants/oxidants available for final chemical reactions; and (3) the migration distance and the lifetime of photo-excited carriers. Longer distances and shorter lifetimes are obviously undesirable for achieving excellent photocatalytic efficiency.

To meet the above criteria, N^{3-} and M^{5+} (M=Nb, V, Ta) co-doping strategies were designed to develop TiO_2-based VLCs. That is, N^{3-} and M^{5+} ions are simultaneously incorporated into TiO_2 crystal structures by substituting a proportion of the Ti^{4+} and O^{2-} host ions. The atomic orbitals of these extrinsic co-dopant ions will hybridize with that of Ti^{4+}, O^{2-} or each other to extend the light absorption of TiO_2 towards the visible light regime, to reduce the recombination of electron-hole pairs, and finally to enhance VLC efficiencies.

The cation-anion co-doping, in this case N^{3-} and M^{5+} co-doping, leads to the appearance of the third generation of TiO_2-based

Citation: Sun Q, McBride BR, Liu Y. (N^{3-}, M^{5+}) Co-Doping Strategies for the Development of TiO_2-Based Visible Light Catalysts. Res Rev Electrochem. 2017;8(1):106.

photocatalysts. Prior to this, the first generation was designed based on intrinsic TiO_2. Through tuning the exposed crystal plane, particle size distribution, crystal structure, phase compositions, and surface chemistry, the photocatalytic properties of intrinsic TiO_2 could be controlled technologically. However, since this generation of TiO_2 only absorbs ultraviolet light, most of the solar energy spectrum is wasted and their applications are restricted. To increase the light absorption range, the second generation of TiO_2-based VLCs was subsequently developed based on cationic or anionic mono-doping routes. Although most of the elements in the atomic periodic table have been tried, the photocatalytic effects of resultant products are still not good. On one hand, mono-doping cations is difficult to enhance visible light absorption and thus often results in unimproved or even worse visible light catalytic properties. On the other hand, mono-doping anions suffers a technical difficulty in their high doping levels. Furthermore, the generation of "trapping or recombination centers" would also worsen photocatalytic efficiency since they "kill" photo-excited electron and hole carriers. FIG. 1 summarizes the development process, advantages and disadvantages of different TiO_2-based photocatalysts.

This work briefly reviews the recent progress of (N^{3-}, M^{5+}) co-doping strategies for the development of TiO_2-based VLCs. We first explain why N^{3-} and M^{5+} are chosen as co-dopants for TiO_2. Then, we summarize the synthesis methods, material properties, VLC performances and local defect structures of prepared (N^{3-}, M^{5+}) co-doped TiO_2 materials according to the type of used M^{5+} ions. Finally, we point out the existing concerns from current investigations into (N^{3-}, M^{5+}) co-doped TiO_2 materials and prospects for the future development of TiO_2-based VLCs.

The Selection of M^{5+} Cations for Co-Doping with N^{3-} Anions

In (N^{3-}, M^{5+}) co-doped TiO_2 materials, N^{3-} anions are used to substitute O^{2-} ions while M^{5+} cations are used to replace Ti^{4+} ions. The selected M^{5+} ions mainly include Nb^{5+}, Ta^{5+} and V^{5+}. In the atomic periodic table, niobium (Nb) is the 41st element with an electronegativity of 1.6 Pauling units and has the electronic configuration of $1s^22s^22p^63s^23p^63d^{10}4s^24p^64d^45s^1$. Nb ions normally have three chemical valences depending on the number(s) of electrons in 4d and 5s orbitals, i.e., Nb^{5+} (the ionic radius, r_{ion}=0.078 nm in six-coordinated octahedral), Nb^{4+} (r_{ion}=0.082 nm) and Nb^{3+} (r_{ion}=0.086 nm) [1].Tantalum (Ta) is the 73rd element with an electronegativity of 1.5 Pauling units and has the electronic configuration of $1s^22s^22p^63s^23p^63d^{10}4s^24p^64d^{10}4f^{14}5s^25p^65d^36s^2$. Ta^{5+}, Ta^{4+} and Ta^{3+} are their three stable ions at normal conditions. The ionic radii of Ta ions are the same as that of Nb ions (i.e., r_{ion} of Ta^{5+}=0.078; Ta^{4+}=0.082 nm; Ta^{3+}=0.086 nm). Vanadium (V) is the 43rd element with an electronegativity of 1.63 Pauling units and has the electronic configuration of $1s^22s^22p^63s^23p^63d^34s^2$. The ionic radii of V ions are smaller than that of Ta or Nb ions, and are 0.068 (V^{5+}); 0.072 (V^{4+}); and 0.078 nm (V^{3+}), respectively. Since Ta^{5+} and Nb^{5+} ions have almost the similar ionic radius as Ti^{4+} (r_{ion}=0.0745 nm) and their elements show the similar electronegativity to Ti (1.54), they are normally co-doped together with N^{3-} ions into host TiO_2 without generating a large distortion in the local/average crystal structure. The smaller V^{5+} ions are also sometimes

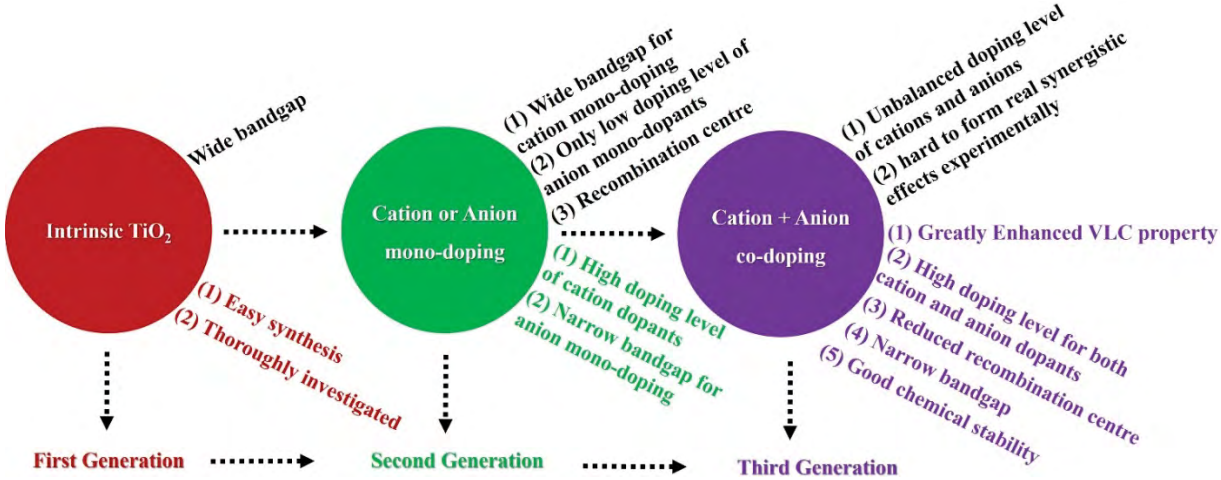

FIG. 1. **The development process, advantages (bottom) and disadvantages (top) of different TiO_2-based photocatalysts.**

chosen as co-dopants due to their easy substitution of Ti^{4+} ions. It is more important that M^{5+} dopant ions lose one additional electron in contrast to the Ti^{4+} host ions. This electron is well compensated by the co-doping of N^{3-} anions. The molar ratio of M^{5+} and N^{3-} co-dopants is thus expected to be 1:1 for the charge balance of the whole co-doped system. Any deviation of the stoichiometric ratio will generate extra Ti^{3+} ions or additional oxygen vacancies. In these two scenarios, (N^{3-}, M^{5+}) co-doping is actually accompanied by N^{3-} or M^{5+} mono-doping.

Two TiO_2 crystal structures, anatase with space group symmetry $I4_1/amd$ and rutile with space group symmetry $P4_2/mnm$, are normally chosen as the host matrices since their syntheses are easier in comparison with other polymorphs. The coupling of N^{3-} and M^{5+} ions in TiO_2 host materials are considered to play three important roles in the enhancement of photocatalytic effects: [2] (1) activating the absorption of lower photon energies; (2) mutually compensating for the additional charges or defects generated by the introduction of dopants; and (3) facilitating a larger total dopant concentration (especially for N^{3-} anions) when N^{3-} and M^{5+} ions are bound together.

Synthesis, Characterization, Photocatalytic Properties and Related Theoretical Calculations of (N^{3-}, Nb^{5+}) Co-Doped TiO_2

Various experimental routes have been tried to date to synthesize (N^{3-}, Nb^{5+}) co-doped TiO_2 materials. TABLE 1 lists the synthesis processes, characterized properties and VLC effects for (N^{3-}, Nb^{5+}) co-doped TiO_2 [3-10,12,13]. The sources of used N are categorized into three types: (1) the colorless liquid HNO_3 (nitric acid), $C_4H_{11}N$ (*n*-Butylamine), NH_4OH (ammonia solution); (2) solid $C_6H_{12}N_4$ (hexamethylenetetramine), CH_4N_2O (urea) or $(NH_4)[NbO(C_2O_4)_2(H_2O)]\bullet nH_2O$ (ammonium niobium oxalate); and (3) NH_3 (ammonia) gas. Meanwhile, the sources of Nb are mainly focused on $NbCl_5$ (niobium pentachloride), $Ti_{1-x}Nb_x$ alloys (titanium-niobium alloys), $C_{10}H_{15}O_5Nb$ (niobium ethoxide) and $(NH_4)[(NbOF_4)(NbF_7)_2$ (ammonium uoroniobate salt). As for the Ti sources, $TiCl_4$ (titanium tetrachloride), Ti metal, $Ti_{1-x}Nb_x$ alloys, $C_{16}H_{36}O_4Ti$ (titanium *n*-Butoxide), $C_{12}H_{28}O_4Ti$ (titanium tetraisopropoxide) are normally used.

Different synthesis methods have been reported for the preparation of (N^{3-}, Nb^{5+}) co-doped TiO_2 materials depending on the selection of raw materials containing N, Nb and Ti elements. A simple approach has been recently demonstrated by Sun et al. [3]. They designed a novel solvothermal reaction route to directly synthesize (N^{3-}, Nb^{5+}) co-doped anatase TiO_2 nanocrystals without any post-sintering treatment by using concentrated HNO_3, $NbCl_5$, $TiCl_4$ and ethanol. Through this reaction route, it is easier to control the doping ratio of N^{3-}/Nb^{5+} and efficiently increase the doping concentration of difficult-dopant N^{3-} ions. This chemical reaction at the atomic level is also one of the most promising ways to guarantee the homogeneous distribution of co-dopants in TiO_2 crystal structures. Experimental and theoretical investigations confirmed that N^{3-} and Nb^{5+} co-dopants should locally form defect-pairs. FIG. 2 shows the TEM image of their synthesized (5.3 at% N^{3-}, 5.6 at% Nb^{5+}) co-doped anatase TiO_2 nanocrystals, the resultant local defect-pair motif, and the decomposition curve of Rhodamine B under only visible light illumination using the defect-pairs modified TiO_2-based VLCs. The formation of local N^{3-}- Nb^{5+} defect-pairs is critical to narrow the band gap to 2.2 eV from ~ 3.1 eV and to significantly enhance VLC efficiency (20 mg/L Rhodamine B solution is almost completely decomposed by loading 1 g/L defect-pair modified TiO_2-based VLCs under visible light illumination).

In addition, a one-step microwave-assisted hydrothermal method was also designed to simultaneously introduce N^{3-} and Nb^{5+} co-dopants into anatase TiO_2 nanoparticles [4,5]. Their bandgaps, however, are too broad (3.1 and 2.8 eV, respectively) for practical applications as VLCs. Another normal synthetic procedure is to firstly prepare Nb mono-doped TiO_2 by sol-gel or anodization treatment, and then to incorporate N dopants through high-temperature nitridation in NH_3 gas [6-10]. The high-temperature nitridation process depends on the diffusion of N ions, leading to only surface co-doping [10] or a gradient distribution of chemical compositions [11]. Moreover, an excess of Nb^{5+} dopants over N^{3-} would introduce a large number of Ti^{3+} ions to balance the charges of the whole material. In fact, these additional dopant ions and associated defects may play a detrimental role on VLC properties when compared with uniform (N^{3-}, Nb^{5+}) co-doping. Additionally, Chadwick et al. [13] designed an aerosol assisted chemical vapor deposition method to directly prepare (N^{3-}, M^{5+}) co-doped TiO_2 films by using *n*-butylamine and niobium ethoxide. The co-doping level of N^{3-} ions are proven to be too low (only 0.09 at. %) to strengthen the light absorption behaviors and visible light catalytic properties.

TABLE 1. **The synthesis processes, characterized properties and VLC effects for (N^{3-}, Nb^{5+}) co-doped TiO_2 (NP: Nanoparticle; NTA: Nanotube Array; RhB: Rhodamine B; MB: Methylene Blue; 4-CP: 4-Chlorophenol).**

Synthesis				Characterization					VLC properties				
N source	Nb source	Ti source	Method & Condition	N (at.%)	Nb (at.%)	Phase	Bandgap (eV)	Shape	Light source	Dye (mg/L)	VLCs (g/L)	C/C_0 (%)	Ref.
HNO_3	$NbCl_5$	$TiCl_4$	Solvothermal (200 °C, 12 h)	5.3 (XPS, TGA, N-O determinator)	5.6 (XPS)	Anatase	2.2	NP (<10 nm)	Xe lamp (500W, > 400nm, 10 cm)	RhB (20)	1	0@20 min	3
NH_4OH/ CH_4N_2O	$NbCl_5$	$Ti(SO_4)_2$	Microwave-assisted hydrothermal	15 (nominal)	10 (XPS)	Anatase	3.1	NP (~9 nm)	halogen lamp (500W, > 400nm)	H_2O	0.4	100 umol/h	4
$C_6H_{12}N_4$	$NbCl_5$	$TiCl_4$	Microwave-assisted hydrothermal (190 °C, 0.5 h)	-	2 (EDX)	Anatase	2.8	NP	LED lamps	NO (2ppm)	-	31%	5
NH_3	$NbCl_5$	$C_{16}H_{36}O_4Ti$	Sol-gel & Post-sintering (500 °C, 5 h, NH_3)	-	1-33.3 (nominal)	Anatase	2.0	NP (20 nm)	Xe lamp (150W, AM 1.5G filter)	MB (40)	-	7@120 min	6,7
NH_3	$NbCl_5$	$C_{16}H_{36}O_4Ti$	Sol-gel & Post-sintering (500 °C, 5 h, NH_3)	0.2 (XPS)	25 (XPS)	Anatase	2.2	NP (20 nm)	xenon lamp (150W, AM 1.5G filter)	H_2O	1	7umol/h	8
NH_3	$Ti_{1-x}Nb_x$	Ti1-xNbx	Anodization & Post-sintering (450 °C, 0.5 h,NH_3)	8.2 (XPS)	10 (nominal)	Anatase	2.8	NTA	halogen lamp (3.0mW/cm^2, > 400nm)	MB (2)	-	12@120min	9
NH_3	$(NH_4)[(NbOF_4)(NbF_7)_2]$	Ti foil	Anodization & Post-sintering (550 °C, 2 h, NH_3)	6.9 (XPS)	4 (bulk)	Anatase	-	NTA	Oriel EmArc (200W)	-	-	-	10
NH_4OH & HNO_3	$NbCl_5$	$C_{12}H_{28}O_4Ti$	Sol-gel & Post-sintering (400 °C, 3 h, air)	-	0.5	Anatase	2.98	NP	xenon lamp (300W, > 420nm)	4-CP	1	0@120 min	12
$C_4H_{11}N$	$C_{10}H_{15}O_5Nb$	$C_{12}H_{28}O_4Ti$	Aerosol assisted chemical vapor deposition	0.06-0.09 (XPS)	2-10 (XPS)	Anatase	2.4-3.5	film	-	-	-	-	13

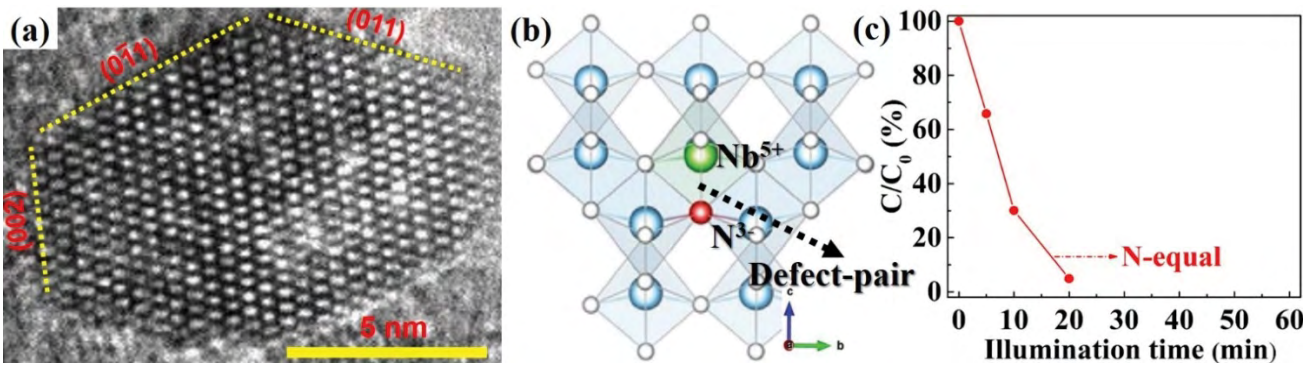

FIG. 2. **(a) The TEM image of (5.3 at % N^{3-}, 5.6 at % Nb^{5+}) co-doped anatase TiO_2 nanocrystals, (b) the resultant local defect-pair motif and (c) the decomposition curve of Rhodamine B under only visible light illumination using these defect-pairs modified VLCs. Copyright Wiley-VCH Verlag GmbH & Co. KGaA. Reproduced with permission from reference 3.**

It can be further seen from TABLE 1 that nearly all of the synthesized (N^{3-}, Nb^{5+}) co-doped TiO_2 materials have an anatase crystal structure. The reported morphologies refer to 0-D nanoparticles with different average particle sizes, 1-D nanotubes and 2-D films. The doping concentrations of N^{3-} and Nb^{5+} co-dopants are usually analyzed by XPS (X-ray photoelectron spectroscopy). Confusion has arisen on the correct XPS core levels of interstitial, substitutional or contaminated N in (N^{3-}, Nb^{5+}) co-doped TiO_2 materials. Moreover, XPS can only provide chemical information on sample surfaces. It is thus hard to quantitatively describe the doping levels of N^{3-} ions and further distinguish the "surface co-doping" or "bulk co-doping" by just relying on the XPS analysis. The combination of XPS with TGA-DSC (thermogravimetry and differential scanning calorimetry analysis) and N-O determinator measurements should give a more reasonable and more acceptable conclusion on the real N^{3-} doping concentration [3].

The decomposition of dyes like Rhodamine B (RhB), methylene blue (MB) and 4-chlorophenol (4-CP) under visible light was measured to present the VLC efficiency of (N^{3-}, Nb^{5+}) co-doped TiO_2. Water splitting experiments were also conducted by some researchers. Due to the different experimental setup and operations such as the light sources, the dye concentrations and types, or the VLCs loading amounts, it is difficult to compare the VLC efficiency of (N^{3-}, Nb^{5+}) co-doped TiO_2 achieved by different researchers. However, one commonly accepted fact is that (N^{3-}, Nb^{5+}) co-doping is more efficient in the enhancement of VLC properties than N^{3-} or Nb^{5+} mono-doping.

Synthesis, Characterization, Photocatalytic Properties and Related Theoretical Calculations of (N^{3-}, Ta^{5+}) Co-Doped TiO_2

In the synthesis of (N^{3-}, Ta^{5+}) co-doped TiO_2 materials, the synthesis methods, experimental processes and utilized Ti/N sources are very similar to that of (N^{3-}, Nb^{5+}) co-doped TiO_2, just with a replacement of the Nb sources with Ta sources. The selected Ta sources include $TaCl_5$ (tantalum pentachloride), Ta metal, $(Ta_2O_5)_{0.01}(TiO_2)_{0.99}$ ceramic pellets, $C_{15}H_{35}O_5Ta$ (tantalum isopropoxide) and $C_{10}H_{25}O_5Ta$ (tantalum ethoxide). TABLE 2 lists the synthesis processes, characterized properties and VLC effects for (N^{3-}, Ta^{5+}) co-doped TiO_2 [14-18]. It can be found that (N^{3-}, Ta^{5+}) co-doped rutile TiO_2 was synthesized by a combination of solvothermal and post-sintering methods [17,18]. During the solvothermal reaction process, Ta mono-doped rutile TiO_2 nanowires or nanorods were first prepared. The subsequent high-temperature nitridation treatment was used to introduce N^{3-} ions into the as-prepared Ta mono-doped rutile nanocrystals to form (N^{3-}, Ta^{5+}) co-doped rutile TiO_2. Comparing with the N mono-doped rutile TiO_2, the co-doping of N^{3-} and Ta^{5+} ions can prohibit the formation of amorphous layers on the nanowire surfaces and thus enhance the incident photon to current conversion efficiency [17]. However, the chemical composition, especially the doping levels of N^{3-} ions, is not discussed at all. It is thus difficult to compare their results with that of co-doped anatase TiO_2 nanomaterials.

The measured bandgaps of (N^{3-}, Ta^{5+}) co-doped TiO_2 materials range from 2.6 to 3.1 eV. It seems that the narrowed band gap can only be achieved at a higher N^{3-} and Ta^{5+} co-doping concentration [14-16]. This conclusion is consistent with the claims of Sun et al.[3] They point out that the higher and nearly equal doping concentrations of cation and anion co-dopants are key to tuning the light absorption behavior and are critical for significantly enhancing VLC properties. Using these synthesized (N^{3-}, Ta^{5+}) co-doped TiO_2, the degradation of MB and oleic acid was characterized under visible light illumination. For example, Zhao et al. [14] investigated the visible light degradation of MB (5 mg/L) under 1 g/L VLCs solution. They found that the C/C_0 (C is the dye concentration at different illumination time and C_0 represents the initial dye concentration) was 31.6% at the reaction period of 240 min. At the same time, Le et al. [15] also investigated the visible light degradation of MB with the same concentration (5 mg/L). The C/C_0 was 7% at the reaction time of 180 min by increasing the loading amount of VLCs to 3 g/L. Due to their different light sources and different loading amounts of VLCs, it is not easy to judge whose VLCs are better for the visible light catalytic decomposition of MB.

Theoretical calculations were performed on (N^{3-}, Ta^{5+}) co-doped TiO_2 to disclose where N^{3-} and Ta^{5+} ions are located in the TiO_2 crystal structure, how the synergistic effects between N^{3-} and Ta^{5+} co-dopants tune the bandgap and affect photocatalytic properties [14,16,19]. FIG. 3 shows a 108-atom super cell containing one substituted N and one replaced Ta. Among various co-doped configurations, N and Ta co-dopants prefer to directly bind together in one octahedron. The extension in the N-Ta distances will lead to higher total formation energy. Actually, N^{3-} and Ta^{5+} co-dopants locally form similar defect-pairs to the N^{3-} and Nb^{5+} co-doping system [3]. The hybridization of N2*p* and Ta5*d* states in N-Ta defect-pairs reduces recombination centers caused by impurity levels (FIG. 3b and 3c), narrows the bandgap, increases carrier mobility, and finally enhances the VLC properties. The calculated band

TABLE 2. **The synthesis processes, characterized properties and VLC effects for (N^{3-}, Ta^{5+}) co-doped TiO_2 (NP: Nanoparticle; NW: Nanowire; NR: Nanorod; MB: Methylene Blue).**

Synthesis				Characterization						VLC properties			
N source	Ta source	Ti source	Method & Condition	N (at.%)	Ta (at.%)	Phase	Bandgap (eV)	Shape	Light source	Dye (mg/L)	VLCs (g/L)	C/C_0 (%)	Ref.
CH_4N_2O	$TaCl_5$	$C_{16}H_{36}O_4Ti$	Sol-gel & Post-sintering (500 °C, 1 h, air)	13.4 (XPS)	12.8 (XPS)	Anatase	2.68	NP	Xe lamp (500W, > 420nm)	MB (5)	1	32@240min	14
NH_4OH	Ta	$C_{12}H_{28}O_4Ti$	Hydrothermal & Post-sintering (300 °C, 1 h, air)	1.7 (XPS)	0.29 (XPS)	Anatase	2.85	NP (20 nm)	Hg-Xe lamp (500W, > 420nm)	MB (5)	3	~7@180 min	15
N_2	$(Ta_2O_5)_{0.01}(TiO_2)_{0.99}$	Ti & $(Ta_2O_5)_{0.01}(TiO_2)_{0.99}$	Magnetron sputtering (400 °C)	0.5-0.6 (XPS)	2.3-1.3 (XPS)	Anatase	3.07-3.16	Film	Xe lamp (420-500nm)	Oleic acid	-	11@120 min	16
NH_3	$C_{15}H_{35}O_5Ta$	$TiCl_4$	Solvothermal & Post-sintering (500 °C, 2 h, NH_3)	-	0.29 (XPS)	Rutile	-	NW	Visible light (>420 nm)	-	-	-	17
NH_3	$C_{10}H_{25}O_5Ta$	$C_{12}H_{28}O_4Ti$	Microwave-assisted solvothermal & Post-sintering (350 °C, 1 h, NH_3)	-	-	Rutile	~2.6	NR	Xe lamp (500W, > 420nm)	H_2O	0.5	0.7 umol h^{-1}	18

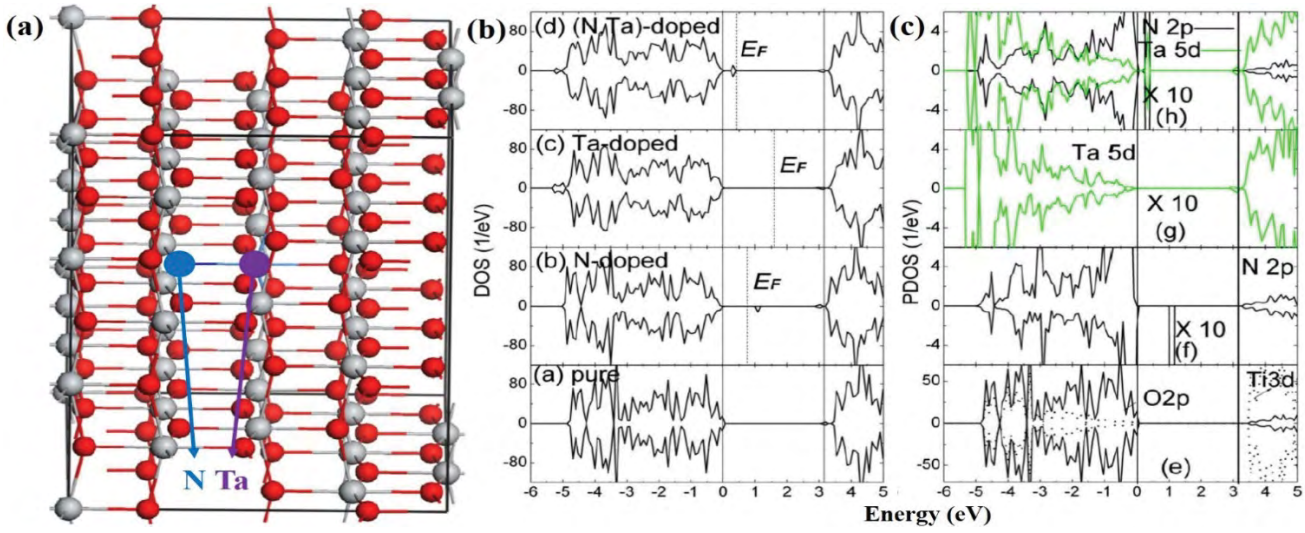

FIG. 3. **(a) A 108-atom supercell containing substituted N and Ta co-dopants, (b) the calculated total DOS and (c) PDOS of un-doped, Ta mono-doped, N mono-doped and (N, Ta) co-doped anatase TiO_2. Reprinted with permission from reference 19.**

gap of 2.7 eV is also consistent with the experimental results [14,18]. For (N^{3-}, Ta^{5+}) co-doped rutile TiO_2, there are no associated theoretical calculations to date.

Synthesis, Characterization, Photocatalytic Properties and Related Theoretical Calculations of (N^{3-}, V^{5+}) Co-Doped TiO_2

The synthesis methods used for the preparation of (N^{3-}, V^{5+}) co-doped TiO_2 materials are the same as that of (N^{3-}, Nb^{5+}) and (N^{3-}, V^{5+}) co-doped TiO_2. For example, the high-temperature nitradation in NH_3 is also used to introduce N^{3-} ions into as-prepared V mono-doped TiO_2. TABLE 3 lists the synthesis processes, characterized properties and VLC effects for (N^{3-}, V^{5+}) co-doped TiO_2 [20-25]. NH_4VO_3 is predominantly used as a V source. In contrast to the synthesis of (N^{3-}, Nb^{5+}) and (N^{3-}, V^{5+}) co-doped TiO_2, the hydrothermal route is frequently used to synthesize (N^{3-}, V^{5+}) co-doped TiO_2 [21-25]. It involves the incorporation of N^{3-} or V^{5+} co-dopant ions into the as-prepared V/N mono-doped TiO_2 precursor in a hydrothermal reaction autoclave. This wet chemical reaction

TABLE 3. **The synthesis processes, characterized properties and VLC effects for (N^{3-}, V^{5+}) co-doped TiO_2 (NP: Nanoparticle; NTA: Nanotube Array; RhB: Rhodamine B; MB: Methylene Blue; MO: Methylene Orange; PCP-Na: Sodium Pentachlorophenate; CAP: Chloramphenicol).**

Synthesis					Characterization					VLC properties			
N source	V source	Ti source	Method and Condition	N (at.%)	V (at.%)	Phase	Bandgap (eV)	Shape	Light source	Dye (mg/L)	VLCs (g/L)	C/C_0 (%)	Ref.
$C_6H_{15}N$	NH_4VO_3	$C_{16}H_{36}O_4Ti$	Sol-gel & Post-sintering (450 °C, 2 h, air)	4 (nominal)	2 (nominal)	Anatase	2.3	NP (7nm)	Xe lamp (150W, 15cm)	RhB (95.8)	0.29	0@60min	20
$C_6H_{15}N$	NH_4VO_3	$Ti(SO_4)_2$	Two-step hydrothermal (180 °C, 22h)	3.12 (XPS)	1.0 (ICP) & 0.5 (XPS)	Anatase	2.5	NP (13nm)	Xe lamp (400W, > 400nm)	PCP-Na (20)	0.4	~20@120 min	21
$C_6H_{15}N$	V^{4+}	$C_{16}H_{36}O_4Ti$	Two-step hydrothermal (180 °C, 22h)	-	-	Anatase	2.8	NP (5nm)	Xe lamp (400W, > 400nm, 25cm)	MB (1.6)	-	80@275 min	22
NH_4VO/ NH_3OH	NH_4VO_3	TiO_2	Hydrothermal (180 °C, 12 h)	2.97 (XPS)	20 (nominal)	Anatase	-	NP (11nm)	Xe lamp (300W, > 420nm)	MO (3.3)	-	54.3@300 min	23
NH_4VO_3	NH_4VO_3	N-TiO_2	Hydrothermal (180 °C, 5 h)	3.4 (XPS)	4.2 (XPS)	Anatase	2.3	NTA	Hg lamp (300W, > 420nm)	CO_2	-	64.5 ppm h^{-1} cm^{-2}	24
$C_6H_{15}N$	NH_4VO_3	$C_{16}H_{36}O_4Ti$	Sol-gel & Hydrothermal (180 °C, 20 h)	0.62 (XPS)	2 (nominal)	Anatase	2.5	NP	Halide lamp (400W, > 420nm	CAP (25)	1	325x10^{-4} min^{-1}	25

route avoids the traditional high-temperature nitridation treatment and reduces the agglomeration of nanoparticles. However, it is debatable whether the dopants can be efficiently diffused into TiO_2 crystal structures at such mild reaction conditions and whether the "surface co-doping" dominates the photocatalytic properties.

Most of the measured bandgaps are around 2.3 and 2.5 eV for (N^{3-}, V^{5+}) co-doped TiO_2. This means that N^{3-} and V^{5+} co-doping can efficiently lower the bandgap and extend the light absorption to visible light regime. In almost all (N^{3-}, V^{5+}) co-doped samples prepared using NH_4VO_3 as raw materials, V^{5+} and V^{4+} ions are found to co-exist. If NH_4VO_3 is replaced by V^{4+}-containing raw material, V^{4+} and V^{3+} will co-exist in the samples. The reasons for the easy reduction of V ions remain unclear to date. The VLC properties of (N^{3-}, V^{5+}) co-doped TiO_2 were characterized through decomposing MB, MO (methylene orange), RhB and 4-chlorophenol; or reducing CO_2 into CH_4. In addition, Eswar et al. [25] used their synthesized (N^{3-}, V^{5+}) co-doped TiO_2 to treat antibiotics/bacteria and found that (N^{3-}, V^{5+}) co-doping would strengthen VLC properties comparing with N^{3-} or V^{5+} mono-doping. The key roles of (N^{3-}, V^{5+}) co-doping on the enhancement of VLC properties are also emphasized by other related researchers.

Theoretical calculations on (N^{3-}, V^{5+}) co-doped TiO_2 demonstrate that (N^{3-}, V^{5+}) co-doping can efficiently enhance VLC properties. FIG. 4 presents the co-doping positions of N and V in anatase TiO_2 and the calculated total DOS (density of states). Here, N^{3-} and V^{5+} chemically bind together to form defect-pairs, again. The formation of defect-pairs narrows the band gap by about 0.45 eV through providing an acceptor level of about 0.33 eV above the valence band and a donor level of about 0.12 eV below the conduction band

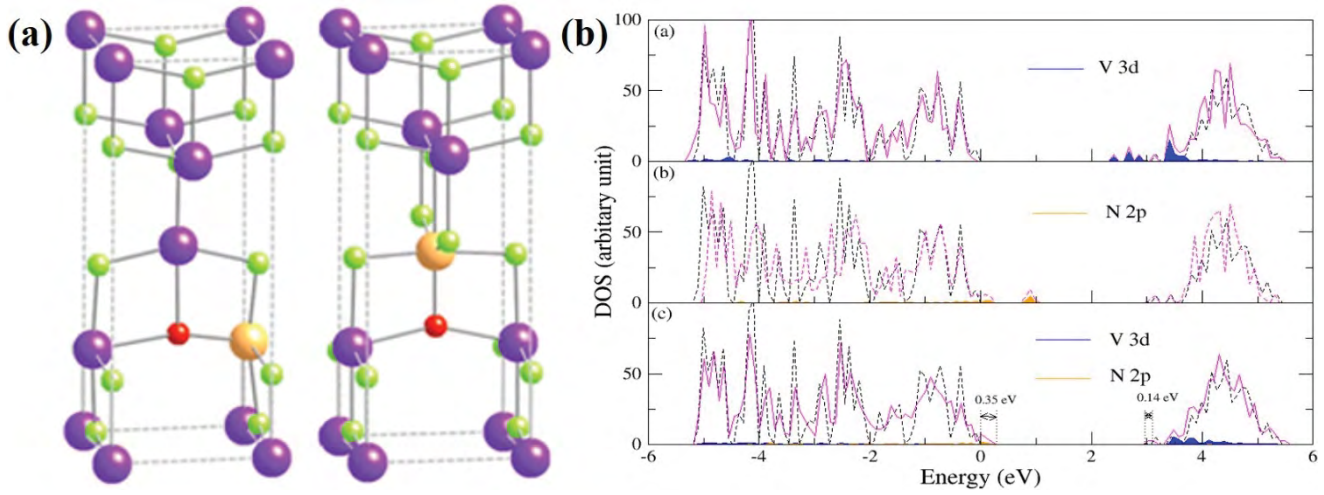

FIG. 4. **(a) The schematic illustration of (N, V) defect-pair configurations in anatase TiO_2 and (b) the calculated total DOS. The orange and red balls represent the co-doped Ta and N, respectively. Reprinted with permission from reference 26.**

[26]. Furthermore, the N-V defect-pairs have a large binding energy of about 0.77 eV, making them rather stable against separation. However, it is a technological challenge to experimentally control the chemical valences of V^{5+} dopants.

Conclusions and Prospects

In (N^{3-}, M^{5+}) co-doped TiO_2 materials, the introduced N^{3-} and M^{5+} ions would chemically bind together to form local defect-pairs. These defect-pairs are critical to narrow the bandgap of host TiO_2, reduce the "trapping or recombination centers" of photo-generated carriers, increase the doping levels of difficult-dopant N^{3-} ions, and thus significantly enhance visible light catalytic properties. Since Nb^{5+} and Ta^{5+} ions are stable in contrast to V^{5+}, it is better to select them as the co-dopants of N^{3-} ions. Given the difficulty in comparing and analyzing the photocatalytic effects reported by different research groups,

(1) A standard photocatalytic reaction setup and conditions should be developed and followed. It would include the used light source, the light illumination intensity, a fixed dye type and concentration, identical loading amounts of the catalysts, and identical reaction times;

(2) At the very least, commercial Degussa P25 should be used as a reference and all experimental results should be quantitatively compared with it;

(3) The chemical compositions of the synthesized samples should be carefully analyzed to easily unveil the intrinsic origin of observed photocatalytic activities.

Based on local defect structure design, it is expected that co-doping TiO_2 with (N^{3-}, M^{5+}) will significantly enhance their VLC properties. The development of defect-pair modified TiO_2-based VLCs is thus beneficial for the highly efficient utilization of clean and renewable solar energy.

REFERENCES

1. The ionic radius and electronegativity of Nb, Ta and V elements and ions can be found from the below website of https://www.webelements.com.
2. Asahi R, Morikawa T, Irie H, et al. Nitrogen-doped titanium dioxide as visible-light-sensitive photocatalyst: designs, developments, and prospects. Chem Rev. 2014;114(19):9824-52.
3. Sun Q, Cortie D, Zhang S, et al. The formation of defect-pairs for highly efficient visible-light catalysts. Adv Mater. 2017;29(11):1605123.
4. Lin HY, Shih CY. Efficient one-pot microwave-assisted hydrothermal synthesis of M (M=Cr, Ni, Cu, Nb) and nitrogen co-doped TiO_2 for hydrogen production by photocatalytic water splitting. J Mol Catal A: Chem. 2016;411:128-37.
5. Zhang P, Yin S, Sekino T, et al. Nb and N co-doped TiO_2 for a high-performance deNOx photocatalyst under visible LED light irradiation. Res Chem Intermed. 2013;39(4):1509-15.

6. Breault TM, Bartlett BM. Lowering the band gap of anatase-structured TiO_2 by coalloying with Nb and N: electronic structure and photocatalytic degradation of methylene blue dye. J Phys Chem C. 2012;116(10):5986-94.
7. Breault TM, Bartlett BM. Composition dependence of TiO_2:(Nb, N)-x compounds on the rate of photocatalytic methylene blue dye degradation. J Phys Chem C. 2013;117(17):8611-8.
8. Breault TM, Brancho JJ, Guo P, et al. Visible light water oxidation using a co-catalyst loaded anatase-structured $Ti_{1-(5\ x/4)}Nb_xO_{2-y-\delta}N_y$ compound. Inorg Chem. 2013;52(16):9363-8.
9. Xu Z, Yang W, Li Q, et al. Passivated n-p co-doping of niobium and nitrogen into self-organized TiO_2 nanotube arrays for enhanced visible light photocatalytic performance. Appl Catal B: Environmental. 2014;144:343-52.
10. Cottineau T, Béalu N, Gross PA, et al. One step synthesis of niobium doped titania nanotube arrays to form (N, Nb) co-doped TiO_2 with high visible light photoelectrochemical activity. J Mater Chem A. 2013;1(6):2151-60.
11. Liu G, Yin LC, Wang J, et al. A red anatase TiO_2 photocatalyst for solar energy conversion. Energy Environ Sci. 2012;5(11):9603-10.
12. Lim J, Murugan P, Lakshminarasimhan N, et al. Synergic photocatalytic effects of nitrogen and niobium co-doping in TiO_2 for the redox conversion of aquatic pollutants under visible light. J Catal. 2014;310:91-9.
13. Chadwick NP, Glover EN, Sathasivam S, et al. Photo-activity and low resistivity in N/Nb co-doped TiO_2 thin films by combinatorial AACVD. J Mater Chem A. 2016;4(2):407-15.
14. Zhao YF, Li C, Hu JY, et al. Ta and N modulated electronic, optical and photocatalytic properties of TiO_2. Phys Lett A. 2016;380:910-6.
15. Le NT, Thanh TD, Pham VT, et al. Structure and high photocatalytic activity of (N, Ta)-doped TiO_2 nanoparticles. J Appl Phys. 2016;120(14):142110.
16. Obata K, Irie H, Hashimoto K. Enhanced photocatalytic activities of Ta, N co-doped TiO_2 thin films under visible light. Chem Phys. 2007;339(1):124-32.
17. Hoang S, Guo S, Mullins CB. Coincorporation of N and Ta into TiO_2 nanowires for visible light driven photoelectrochemical water oxidation. J Phys Chem C. 2012;116(44):23283-90.
18. Nakada A, Nishioka S, Vequizo JJ, et al. Solar-driven Z-scheme water splitting using tantalum/nitrogen co-doped rutile titania nanorod as an oxygen evolution photocatalyst. J Mater Chem A. 2017;23(5): 11710-9.
19. Long R, English NJ. Band gap engineering of (N, Ta)-codoped TiO_2: a first-principles calculation. Chem Phys Lett. 2009 Aug 27;478(4):175-9.
20. Jaiswal R, Patel N, Kothari DC, et al. Improved visible light photocatalytic activity of TiO_2 co-doped with vanadium and nitrogen. Appl Catal B. 2012;126:47-54.
21. Liu J, Han R, Zhao Y, et al. Enhanced photoactivity of V-N codoped TiO_2 derived from a two-step hydrothermal procedure for the degradation of PCP-Na under visible light irradiation. J Phys Chem C. 2011;115:4507-15.
22. Gu DE, Yang BC, Hu YD. V and N co-doped nanocrystal anatase TiO_2 photocatalysts with enhanced photocatalytic activity under visible light irradiation. Catal Commun. 2008;9(6):1472-6.
23. Zhong J, Xu J, Wang Q. Nitrogen and vanadium co-doped TiO_2 mesosponge layers for enhancement in visible photocatalytic activity. Appl Surf Sci. 2014;315:131-7.
24. Lu D, Zhang M, Zhang Z, et al. Self-organized vanadium and nitrogen co-doped titania nanotube arrays with enhanced photocatalytic reduction of CO_2 into CH_4. Nanoscale Res Lett. 2014;9:272.
25. Eswar NK, Ramamurthy PC, Madras G. Novel synergistic photocatalytic degradation of antibiotics and bacteria using V-N

doped TiO_2 under visible light: The state of nitrogen in V-doped TiO_2. New J Chem. 2016;40:3464-75.

26. Phattalung SN, Limpijumnong S, Yu J. Passivated co-doping approach to bandgap narrowing of titanium dioxide with enhanced photocatalytic activity. Appl Catal B. 2017;200:1-9.